WELDING RESEARCH

SUPPLEMENT TO THE WELDING JOURNAL, APRIL, 1983

Sponsored by the American Welding Society and the Welding Research Council

Lamellar Tearing in Fillet Weldments of Pressure Vessel Fabrications

Investigation of two distinct modes of crack propagation in cracked pressure vessel fillet welds leads to development of a method to evaluate susceptibility to plate cracking

BY A. D. HATTANGADI AND B. B. SETH

ABSTRACT. Fractographic analyses of several cracked weldments from pressure vessel fabrications of ASTM A515 Grade 65 carbon steel plates are presented. Two distinct modes of plate cracking – classical lamellar tearing and abrupt brittle fracture – are observed.

A model using the fracture mechanics approach is developed to explain the two modes of cracking. Based on this, a screening criterion for the plates using conventional tensile and Charpy impact tests in the through-thickness direction of the plates is proposed.

Introduction

Lamellar tearing has gained increasing interest from both the steel making industry and the fabrication industry. The phenomenon of lamellar tearing is defined typically by pull-out fractures which occur when rolled steel plates are joined by means of multi-run fillet welds. Strains develop as a result of these welds in the thickness direction of the plates. If these strains are large enough, fractures occur in the material near the weld preferentially, following the laminated inclusions in the rolled plates.

Considerable study has been done on lamellar tearing (Ref. 1-3) to verify the effects of plate quality, welding parameters and structural design factors. However, this has primarily been limited to the use of small scale simulated weld tests.

Sufficiently high constraints can be developed in such tests through the proper use of specimen design, welding sequence and other related welding parameters. D. Elliott (Ref. 3) has reported micromechanisms of the lamellar tears only through the use of such simulated weld tests. In his paper, he deals with the relationship between fracture propagation and the micromechanisms of lamellar tearing.

The main disadvantage of such tests is that they frequently exhibit only the lamellar tearing mode of fracture. In reality, however, when structural parts of massive weight and dimensions are subject to large welding strains and mechanical constraints, a brittle mode of fracture appears in addition to the lamellar tearing. So when one considers the potential for cracking during welding, both these modes of cracking should be evaluated.

The intent of this paper is to describe these two distinct modes of fracture – namely, lamellar tearing coupled with brittle fracture. Details of fractographic examination are presented for subsequent analysis. A model based on the fracture mechanics approach is proposed to explain the two modes of cracking. The model further lends itself to making engineering estimates on the critical size of lamellar tears. These are compared with the actual sizes typically observed in the weldments.

The paper also discusses how the through thickness tensile ductility and Charpy V-notch impact strength can effectively be used to evaluate the susceptibility of plates to lamellar tearing.

Table 1—Details of Weldment Examined

Weldment identification	Plate thickness, in.[a]	Material	Location of tear	Tear length, in.[a]	Welding process
A	3	ASTM A 515 GR65 steel	0.25 in. from fillet weld edge	10	Submerged arc
A1	3	ASTM A 515 GR65 steel	0.25 in. from fillet weld edge	24	Submerged arc
A2	4	ASTM A 515 GR65 steel	0.25 in. from fillet weld edge	40	Submerged arc
B	3.25	ASTM A 515 GR65 steel	0.125 in. from weld edge	20	Submerged arc
C	2.50	ASTM A 515 GR65 steel	Fillet weld edge	49	Gas metal arc

[a] 1 in. = 25.4 mm.

A. D. HATTANGADI and B. B. SETH are with the Steam Turbine-Generator Divisions of the Power Generation Group for Westinghouse Electric Corporation, Philadelphia, Pennsylvania.

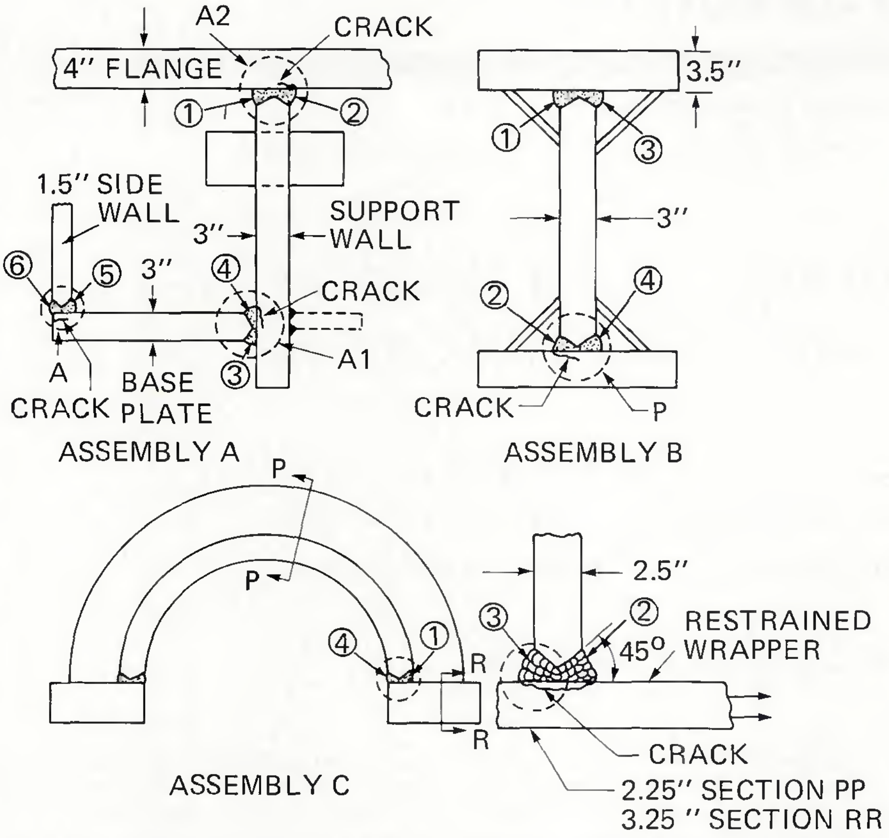

Fig. 1 — Three weldments showing crack locations. Numbers in circles represent normal welding sequence

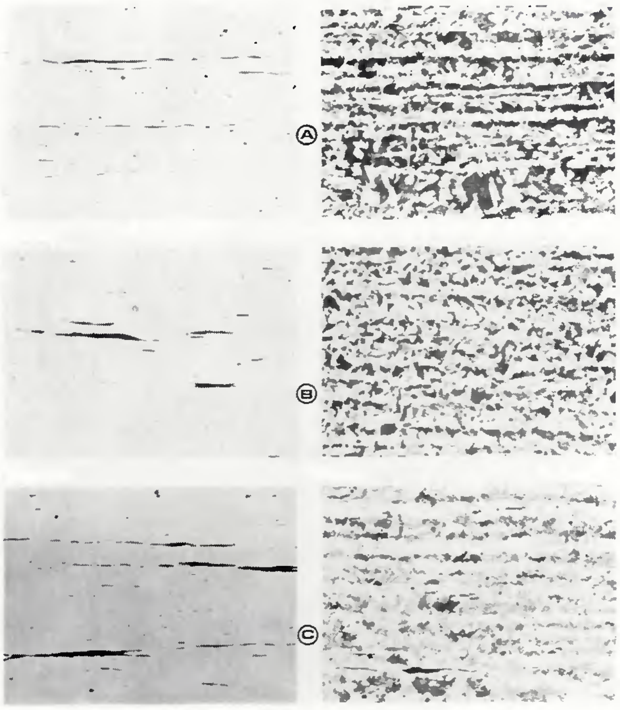

Fig. 2 — Cleanliness (left) and microstructure (right) of cracked plates: A — plate for assembly A; B — plate for assembly B; C — plate for assembly C. X100 (reduced 61% on reproduction)

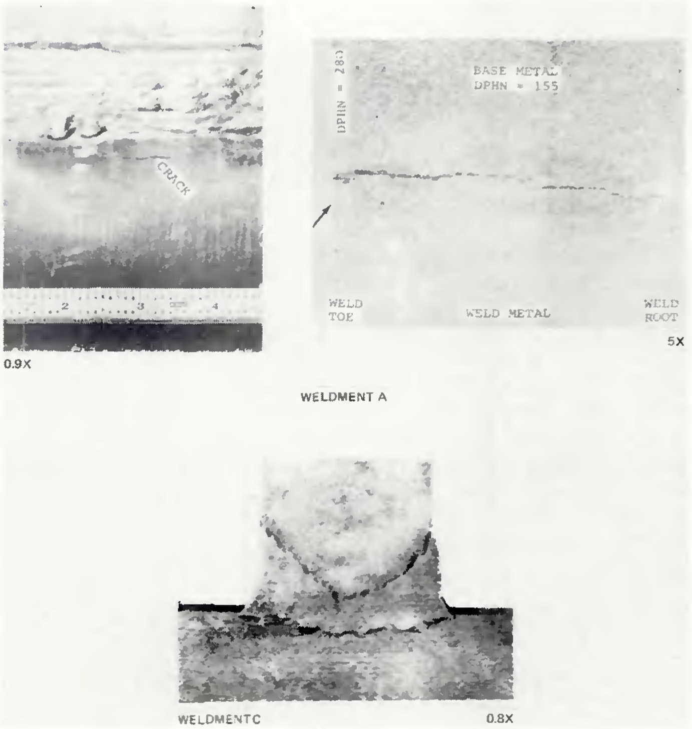

Fig. 3 — Transverse sections through cracked weldments (reduced 57% on reproduction)

Examination of Failed Weldments

Background Information on Cracked Weldments

Three different types of weldment assemblies used in the manufacture of pressure vessel fabrications were examined for fractographic investigation. Schematic representation of these weld joints with their respective crack locations are shown in Fig. 1.

Weldment assemblies B and C in Fig. 1 ranged from 6 to 8 ft (1.8 to 2.4 m) in size. On the other hand, assembly A was a more complex fabricated structure with dimensions ranging up to 30 ft (9.1 m). A small portion highlighting crack locations in assembly A is, therefore, shown. Subassembly C, being relatively smaller in size, was welded with gas metal arc, while the other two were submerged arc welded at higher heat inputs and rates of welding.

The massive size and weight of these fabrications shown in Fig. 1 offered considerable mechanical constraints to the various weldments. These coupled with welding strains produced cracks under the weldments as long as 49 in. (1.24 m) in some cases. Table 1 lists the extent of such cracking in the weldments as seen on the surface of the cracked plates. Weldments A and B with L joint design showed cracks up to 0.25 in. (6.4 mm) removed from the outer edge of the fillet weld, whereas weldment C revealed cracking right along the toe of the weld.

The cracked plates employed in the weldments were made of carbon steel to

ASTM A515 Grade 65 specifications. Table 2 lists the chemical composition and in-plane mechanical properties of these plates as compared with the ASTM A515 Grade 65 carbon steel specifications. The identity of the rolling direction of the original plates was not retained. Therefore, the in-plane tests could be at an angle ranging from 0 to 90 deg from the rolling direction.

Figure 2 shows unetched and etched microphotographs of the plates with their typical inclusion content and microstructures. Note the long rolled-out inclusions. These were later identified to contain Mn, S, Al, and Si. All of the microstructures show the relatively coarse grain size of the plates typical of the Si deoxidation practice employed in their manufacture. Also, while the plates were given a normalizing heat treatment, the samples show varying degrees of ferrite-pearlite banded structure.

Table 2—In-Plane Properties of Cracked Plates

Mechanical	ASTM A 515 GR65 Steel	Cracked plates
Tensile strength, ksi[a]	65–77	66–77
Fracture strength, ksi	–	110–162
0.2% yield strength, ksi	35 min.	35–45
Elongation in 8 in., %	19 min.	–
Elongation in 2 in., %	23 min.	24–39
Charpy V-notch energy, ft-lb[b]	–	39–50
Test orientation	In plane	In plane
Number of tests	1/plate	5/plate
Chemical, %		
C (max)	0.33	0.26–0.31
Mn (max)	0.90	0.77–0.90
P (max)	0.035	0.003–0.017
S (max)	0.040	0.023–0.028
Si	–	0.19–0.26

[a] ksi × 6.894757 = MPa.
[b] ft-lb × 1.355818 = J.

Metallographic and Fractographic Examination

Large sections of the cracked weldments were selected for further fractographic investigation. Two such typical cross sections are shown in Fig. 3 for weldments A and C. In the case of weldment A, the crack lies primarily in the base metal. Weldment C, on the other hand, shows cracking in the heat-affected zone. Also, note the large separation in the crack at the weld toe in weldment A. This is indicative of the high strains in that area.

A magnified view of the circled area from weldment C is presented in Fig. 4B. The micrograph shows classical lamellar tearing morphology (Ref. 1). As the weld strains normal to the plate thickness increase, decohesion between the "lamellar" inclusion and matrix takes place at the interface. This results in formation of elongated voids. Such voids adjacent to each other later join with increasing constraint on the weldment by a shear wall. This is shown schematically in Fig. 4A. While these shear walls are generally transgranular, some evidence of their intergranular nature could be seen in Fig. 4C.

Due to the rather discontinuous nature of cracking, these weldments had to be sectioned further. Such small sections from each weldment were opened for fractographic examination. This procedure made the task of identifying crack initiation difficult.

Optical inspection of the fractures at low magnification showed a typical blend of fibrous patches with woody appearance and large shiny, granular areas. The fibrous patches, darker in color, were characteristic of lamellar tears. Their darker shade in contrast to the surrounding granular areas suggest that these were the primary fractures sites. One such area from weldment C is shown in Fig. 5. This shows an elliptical lamellar tear about 0.15 in. (3.8 mm) wide and 1 in. (25.4 mm) long in the background of granular fracture.

Further fractographic work was concentrated in identifying fracture features in the lamellar tear and the granular areas. A scanning electron miscroscope (SEM) was used to examine the fracture surfaces. For the sake of interpreting details of lamellar tear as seen on the SEM, one must be familiar with its schematic representation shown in Fig. 6A. With increasing welding strains and mechanical constraint, rolled-out elongated inclusions decohese from the adjacent matrix material, forming elongated voids. The main reason for the elongated inclusions to decohese at their interfaces in preference to globular inclusions is the relatively lower surface energy associated with them (Ref. 4). Voids thus formed join

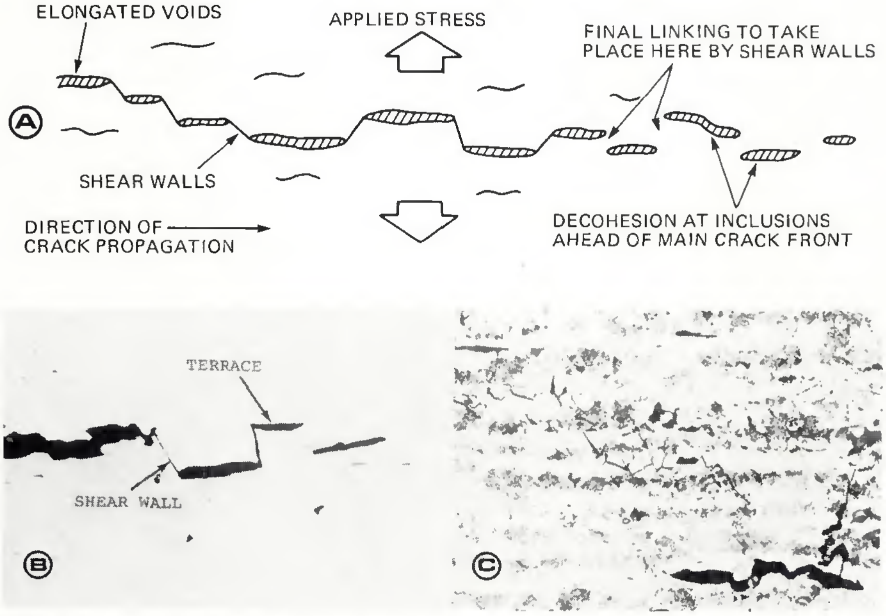

Fig. 4—Details of lamellar tear from weldment C: A—schematic of lamellar tear formation; B—magnified view of circled area in Fig. 1 assembly C; C—evidence of intergranular nature of shear walls. B and C—X100 (reduced 43% on reproduction)

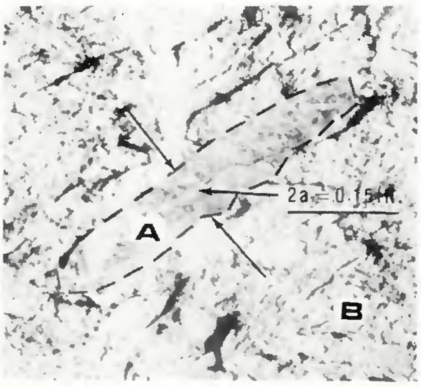

Fig. 5—Typical fracture surface from weldment C. A—patch of lamellar tear; B—brittle fracture. X2.5 (reduced 28% on reproduction)

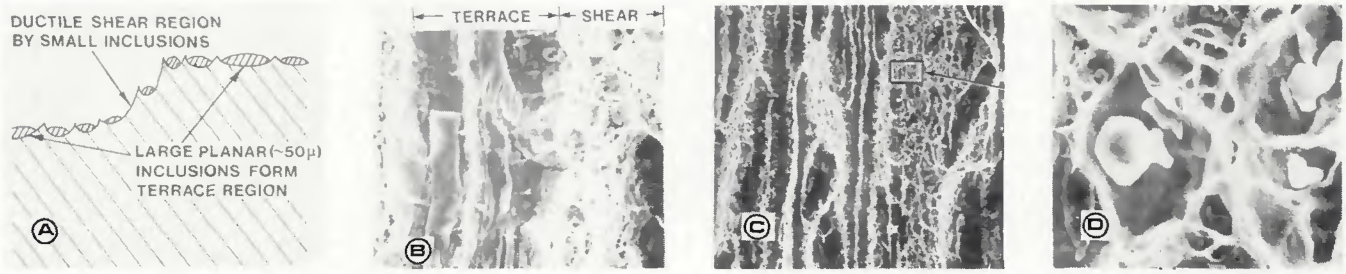

Fig. 6 — Fractographic details of lamellar tear from weldment C: A — schematic representation of lamellar tear; B — fractographic features corresponding to micromechanisms; C and D — elongated inclusions in terrace region enclosed by equiaxed dimples containing globular inclusions. B — X800, C — X600, and D — X600 (all reduced 49% on reproduction)

each other to form horizontal "terrace" regions. Such regions are developed at several different locations along the length and the width of the weldment.

With additional welding strains, shear deformation occurs in the areas separating the terrace regions. This involves relatively smaller inclusions, ($\sim 5\mu$) through localized ductile deformation. Such regions are defined as "shear walls"; they consist of small ductile dimples.

Fractographic features corresponding to the micromechanisms explained above are shown in Fig. 6B for the lamellar tear from weldment C. Note the elongated strip-like inclusions in the terrace region. These are enclosed by equiaxed dimples containing globular inclusions. This is shown in Figs. 6C and 6D.

Inclusions observed on the terrace regions were analyzed using the energy dispersive x-ray analyzer attachment of the SEM. They were found to contain Mn, Si, S, and Al — Fig. 7. Lighter phase inclusions (rich in Mn and S) are surrounded by darker phase inclusions (rich in Mn, Si and Al). Individual inclusions rich in Mn and Si were also seen in such regions. Globular inclusions located on the shear wall, on the other hand, were found to contain S and small amounts of Al.

Granular fracture surrounding the patch of lamellar tear was then examined on the SEM. Topographical features were typical of low energy brittle fracture. One such area from the weldment C fracture is shown in Fig. 8. The river markings on the transgranular facet indicate the brittle mode of fracture.

While the fractographic features presented in this paper pertain exclusively to the weldment C fracture, similar details were also noted on the others. In all weldment fractures examined, there was definite evidence of two distinct modes of cracking — lamellar tearing and brittle mode of propagation.

Mechanical Properties of Cracked Plates

The plates involved in the three weldment cracks were tested for their mechanical properties in the through-thickness direction. Tensile tests would give a direct measure of the plate ductility. Plate ductility, in turn, is influenced by the inclusion morphology and can therefore be correlated to the lamellar tearing mode of fracture. Charpy impact tests, on the other hand, would simulate the transgranular brittle mode of fracture and relate to the toughness characteristics of the plates.

Buttonhead tensile and Charpy V-notch (CVN) specimens shown in Fig. 9 were machined from the cracked plates

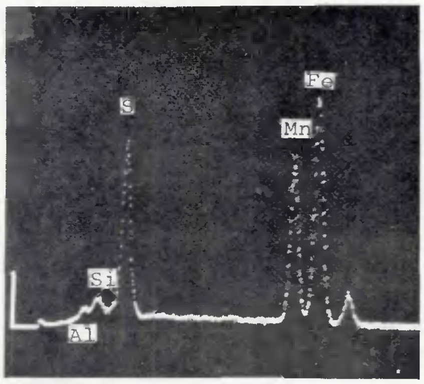

Fig. 7 — EDS spectra of inclusions found in the terrace regions

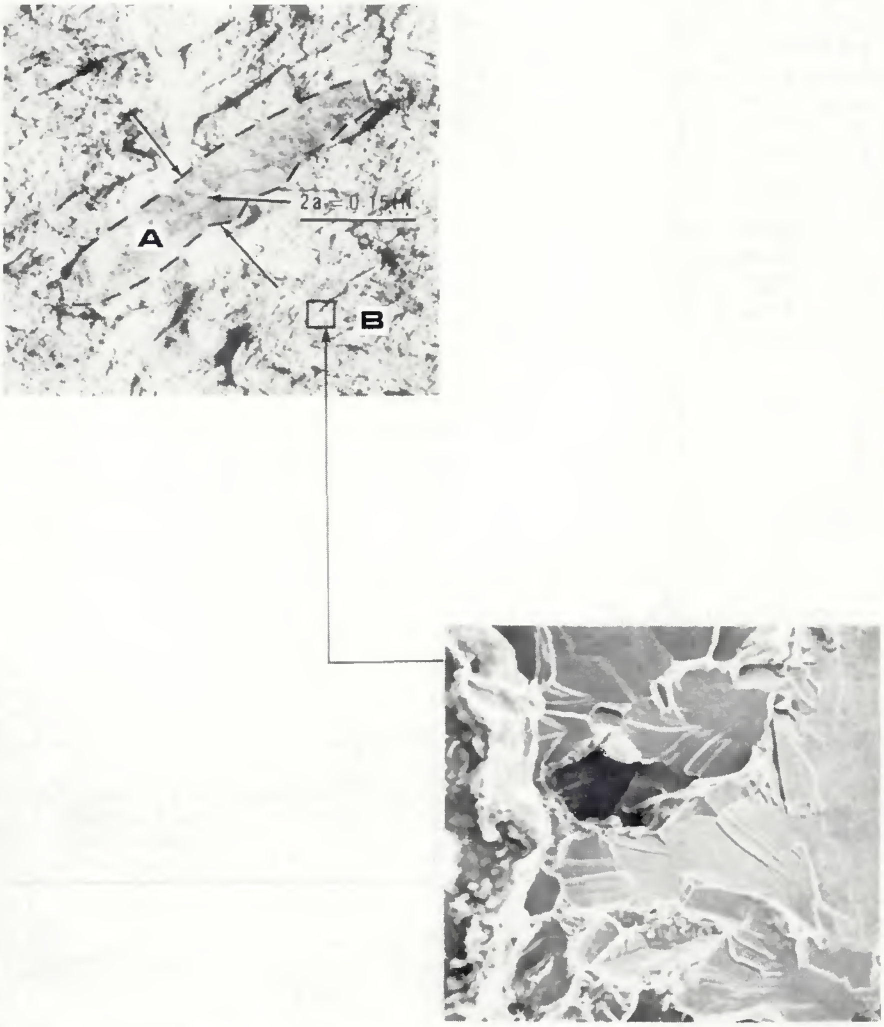

Fig. 8 — SEM fractograph showing brittle mode of crack propagation: top — X2.5; bottom — X500 (both reduced 24% on reproduction)

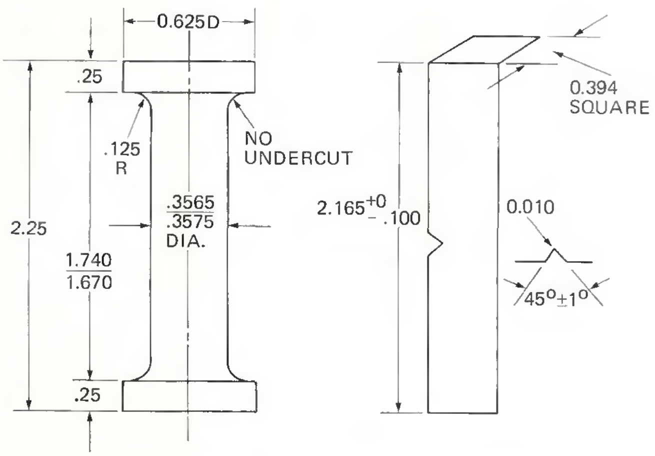

Fig. 9—Tensile and Charpy V-notch impact specimens (dimensions in inches)

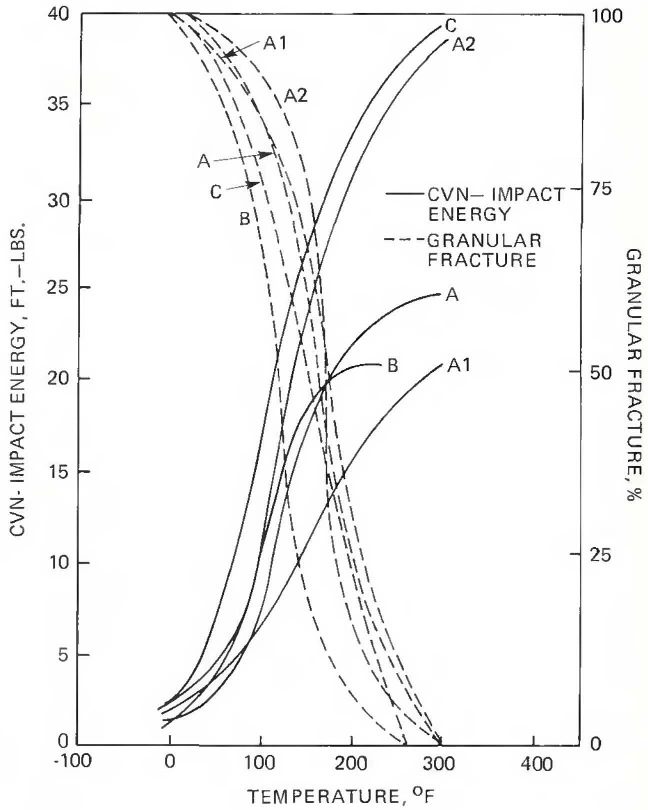

Fig. 10 (right)—Through thickness CVN impact test results for the cracked plates

in the through thickness direction. The notch was machined so that the fracture plane coincided with the cracking plane in actual weldments. Tensile specimens were pulled at ambient temperature in the Universal Instron testing machine at a constant strain rate of 750% per hour. This facilitated computing elongation (a measure of ductility) using two independent techniques—one by the conventional method of putting broken specimens together and measuring the extension of original gage length; the other from noting the overall duration of the test. The two methods showed good agreement to within ±5% of the absolute percent elongation values.

Charpy V-notch impact tests were conducted at ambient and higher temperature in compliance with ASTM E-23. CVN energy vs. temperature and % granular fracture vs. temperature curves were developed for the cracked plates. Results of these mechanical tests are presented in Table 3 and Fig. 10.

While yield and tensile strength values in the through thickness direction of the plates are generally lower than those in the in-plane direction (Tables 1 and 3), substantial difference in the corresponding elongation and reduction in area values can be noted. This is typically indicative of the poor ductility levels of the plates in the through thickness direction. Note that all the plates show FATT (Fracture Appearance Transition Temperature) values above ambient temperature. The room temperature CVN energy values were not only significantly lower than those in the in-plane direction, but were very low. This indicates the relatively low toughness properties of the plates in the through thickness direction.

Ductility parameters (elongation, reduction in area) and toughness values (CVN energy) at ambient temperature are further plotted in Fig. 11. Note that the average elongation and reduction in area values for the cracked plates are less than 12 and 16% respectively, while CVN energy values are longer than 12 ft-lb (16.3J).

Discussion

The metallographic and fractographic investigation of cracked fillet weldments described in this paper suggest two prominent modes of crack propagation—classical lamellar tearing and brittle transgranular mode. Previous investigators (Ref. 1, 3) have not observed the brittle mode of fracture, but have only simulated lamellar tearing through the use of small scale weld tests. Both modes must be accounted for to prevent cracking in components massive in weight and dimensions.

The topographical features of lamellar

Table 3—Through-Thickness Tensile and CVN Properties of Cracked Plates (Ambient Temperature)

Plate identification	Yield strength, ksi[a]	Tensile strength, ksi	Fracture strength, ksi	Elongation, %	Reduction in area, %	CVN energy, ft-lb[b]	FATT, °F[c]
A	34.7-35.9	50.7-73.0	65.2-68.8	6-7	11-17	4-5	160
A1	34.5-35.7	50.2-63.9	54.4-66.1	5-10	7-14	5-10	170
A2	27.1-28.1	—	52.5-70.9	4-9	10-22	6-7	170
B	34.8-35.1	66.8-73.6	68.9-83.3	8-17	7-20	6-7	118
C	35.8-36.2	65.5-65.8	69.8-70.0	7-13	7-12	9-16	150

[a] ksi × 6.894757 = MPa.
[b] ft-lb × 1.355818 = J.
[c] °C = 5/9(°F − 32)

tearing observed on the fractures are very similar to the ones reported earlier by D. N. Elliott (Ref. 3) on simulated weld tests. The preferential decohesion between inclusion and matrix material for manganese silicates and sulfides can be explained on the basis of their shapes. These are elongated, thin inclusions with low surface energy and high stress concentrations at their tips, unlike the globular inclusions. Hence, silicates and sulfides are the prime agents in the formation of terrace regions of the lamellar tear. Globular inclusions, on the other hand, participate in the shear wall formation and subsequent joining of the terrace regions. It is obvious from this mechanism that the non-metallic inclusions play a significant role in the formation of a lamellar tear.

It is not the authors' contention to presume that different types of weld defects such as porosity, slag, hot tears, lack of fusion, etc. may not be crack-initiating sites. These certainly can contribute to crack initiation under high levels of constraint in the weldments. However, the main intent of the fractographic investigation described in this paper was to identify the mechanisms of crack propagation. Due to the enormous sizes of the fractures involved, it was almost an impossible task to pinpoint the crack initiation sites let alone relate them to any kind of weld defects.

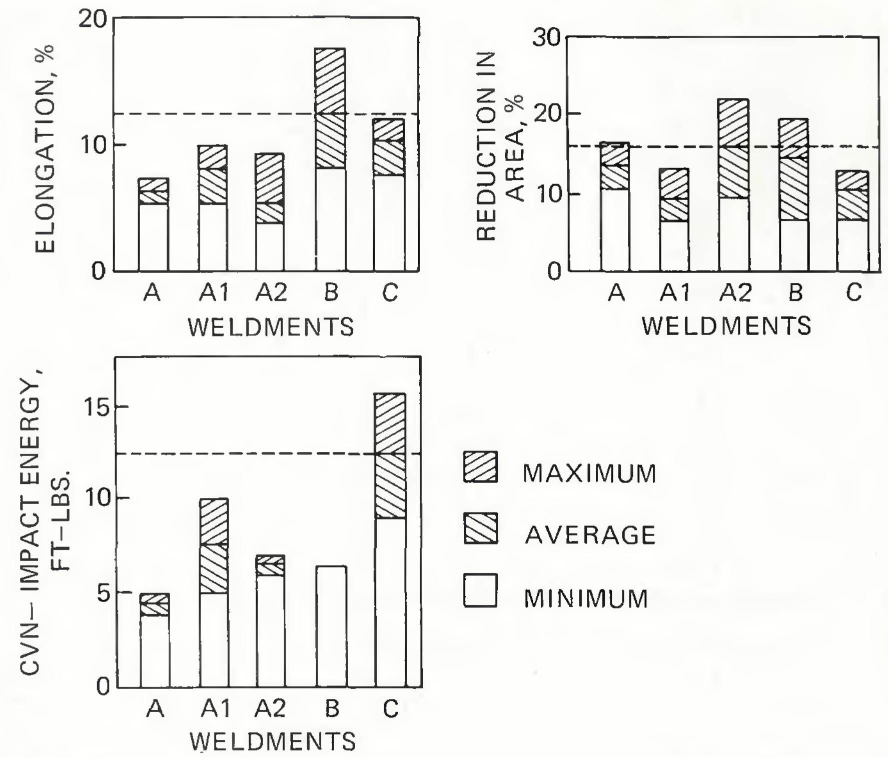

Fig. 11 — Through-thickness tensile and CVN impact data from cracked plates (ambient temperature data)

The darker tinge associated with lamellar tear patches in contrast to the brittle fracture background suggests that lamellar tearing is the initial mode of fracture. It is conceivable that during the cooling process, residual welding strains in addition to mechanical constraint build up under fillet weldments. Several patches of lamellar tears form, when these strains reach sufficiently high level along the length and width of the weldment.

When the patches grow to a critical size tolerated by the welded plates (or the heat-affected zone in the plates, as the case may be), any additional build-up of stresses in such regions causes the weldment to fracture abruptly in a brittle manner. Thus, lamellar tearing can be visualized as a fracture mechanism up to a critical size (subcritical growth) and the

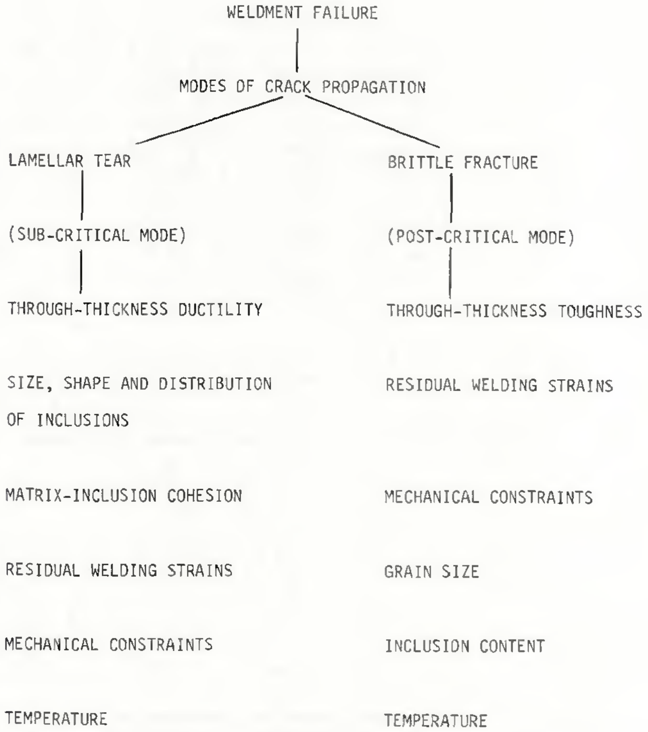

Fig. 12 — Schematic representation of factors affecting weldment cracking

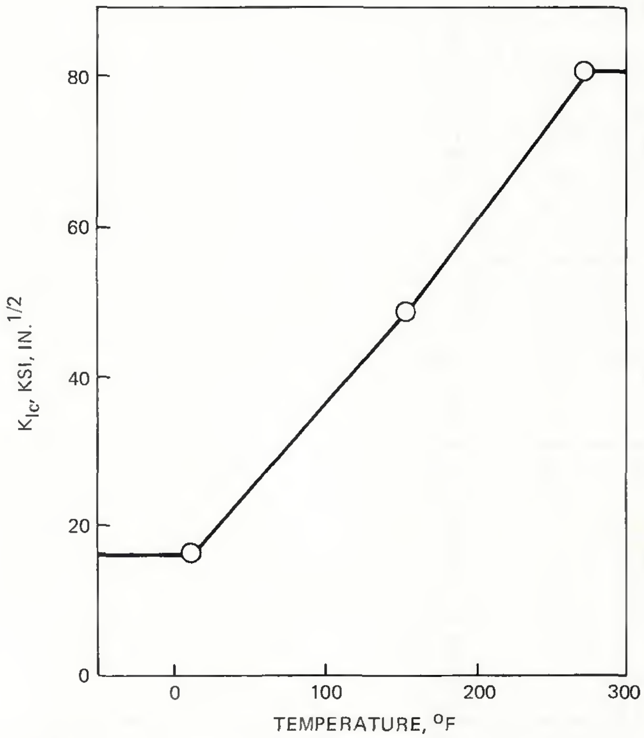

Fig. 13 — K_{Ic} vs. temperature for weldment C based on through-thickness properties

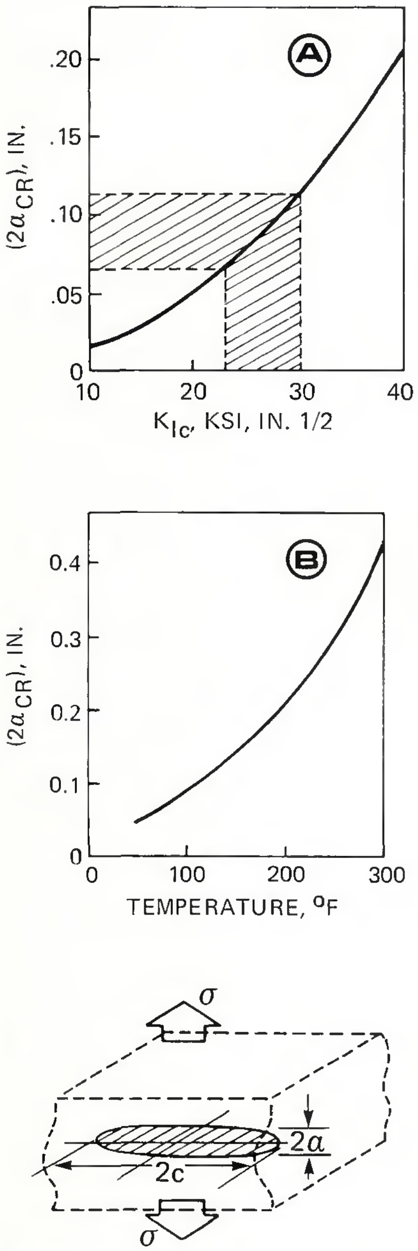

Fig. 14 — Critical lamellar tear sizes plotted as functions of K_{Ic} and temperature: A — K_{Ic}; B — temperature

brittle mode as a mechanism beyond the critical levels of lamellar tears (post-critical growth). Such a model for the analysis of cracking in structures with fillet weldments is further substantiated by all the fractographic observations described in this paper.

Figure 12 shows a schematic presentation of the model. The factors affecting the two modes of fracture are shown here, and are self-explanatory. Some of these factors are discussed below.

1. *Temperature.* It is documented (Ref. 5) that carbon and low-alloy steels generally show a ductility trough around 200 to 400°F (93 to 204°C). Since lamellar tearing is strongly influenced by the plate ductility, it is likely that such tearing occurs in this temperature range. This is further confirmed by Kihara and Nishio (Ref. 6). Minimizing welding strains in this range of temperature can, therefore, reduce the chances of lamellar tearing.

Temperature will also influence the brittle mode of fracture. The toughness of carbon steel increases with temperature; this, in turn, implies a greater resistance to abrupt brittle fracture. Theoretically, therefore, some form of preheat should lessen the susceptibility of the weldment to brittle fracture. (A word of caution on the use of preheat: sectional preheating of large structures may result in abnormal thermal stresses which will not always be beneficial.)

2. *Grain Size.* The grain size of carbon steel plates has an inverse effect.The smaller the grain size, the higher the toughness and lower the chances of brittle fracture. Grain size, of course, depends on the deoxidation practice and thermo-mechanical history of the plates.

Fracture Mechanics Approach

The fracture model proposed above, consisting of subcritical and postcritical modes of fracture for the weldments, lends itself to the use of linear elastic fracture mechanics. One can estimate subcritical lamellar tear sizes before the brittle fracture triggers in. Linear elastic fracture mechanics restricts such analysis only to the elastic stress field at the crack tips; for this reason, it is not accurate for application to lamellar tears. The tears are totally a result of localized plastic deformation in the vicinity of nonmetallic inclusions. While this may be the case, engineering estimates can still be made for the sake of comparison with fractographic observations. Besides, certain corrections such as the triaxial state of stress may be employed to account for the localized plasticity.

With the knowledge of fracture toughness (or plane strain stress intensity, K_{IC}) for the cracked plate steel, one can determine critical sizes of lamellar tears. Begley and Logsden (Ref. 7) have developed a satisfactory method of computing K_{IC} vs. temperature from simple correlations involving conventional tensile and CVN impact properties. Figure 13 shows such a curve developed for weldment C based on the lower bound of through-thickness properties of its plates.

Critical sizes of lamellar tears are calculated from the following equation for an embedded crack in a weldment (Ref. 8):

$$a_{cr} = \frac{K_{IC}{}^2[\phi^2 - 0.212\,(\sigma/\sigma_{ys})^2]}{\pi\,\sigma^2}$$

where a_{cr} = critical lamellar tear, in.; K_{IC} = fracture toughness, ksi-in.$^{1/2}$; σ = applied stress, ksi; σ_{ys} = uniaxial yield strength, ksi; ϕ^2 = shape factor.

Lamellar tear patches being generally elliptical with ratio of major to minor axis greater than 5 (refer to Fig. 5), shape factor ϕ^2 is taken as 1. The localized stresses in the vicinity of the tear are assumed to be equal to $\sqrt{3}$ times uniaxial yield strength of the plate steel because of the triaxial state of stress.

Figure 14A shows critical sizes of elliptical lamellar tears plotted as a function of K_{IC}. A range of 23 to 30 ksi-in.$^{1/2}$ (25.3 to 33 MN $\sqrt[3]{m}$) of K_{IC} values at ambient temperature for cracked plates thus represents a band of critical size ($2a_{cr}$) equal to 0.07-0.12 in. (1.8 to 3 mm). For the weldment C in particular, the critical size ($2a_{cr}$) amounts to 0.12 in. (3 mm); this compares fairly well with the size of lamellar tear patch observed (see Fig. 5).

Figure 14B, on the other hand, shows critical tear sizes as a function of temperature. The curve is established on the basis of the lower bound of K_{IC} values of the cracked plates. Note that the critical size ($2a_{cr}$) increases by a factor of 3 with temperature rising to 200°F (93°C).

All the cracked plates examined did not show individual inclusions as large as those defined by the critical sizes shown in Fig. 14. However, in very poor quality plates, inclusions of such sizes are likely to be present. In a normal situation it is conceived that the growth of the tear occurs only as a result of the linking of several individual inclusions.

Screening Criteria for Steel Plates

Two considerations appear significant from the proposed fracture mechanics model. A plate may withstand yield stresses but one would expect a small amount of plastic strain in the through thickness direction prior to cracking. Thus, lamellar tearing would be a problem if significant plastic strain developed in the base metal during welding. However, if general welding conditions are such that these strains are reduced, cracking may still develop if the fracture toughness for the material is low enough and weld defects larger than critical sizes exist. It is apparent, therefore, that tensile and fracture toughness (or CVN impact) tests in the through-thickness direction would provide a meaningful method of evaluating susceptibility to plate cracking. Since through-thickness properties show a large variation within a plate due to nonuniformity, it is necessary to run several tests.

Figure 11 shows the through-thickness ductility and toughness properties of the cracked plates based on 5 tests per plate. It is reasoned that the highest average value of these properties could be used to develop a screening criterion for such plates. Based on this rationale, the following guidelines can be considered reasonable: T.T. elongation at ambient temperature — 12%; T.T. reduction in area at ambient temperature — 16%; T.T. CVN energy at ambient temperature — 12 ft-lb

(16.3J).

While the rationale for developing the above criteria can generally be applied to similar problems for fillet weldment cracking, the specific property values used above may vary with different applications of the plates. The screening criteria mentioned above are considered valid only for the ASTM A515 Grade 65 carbon steel plate weldments discussed in this paper.

Conclusions

1. Fractographic and metallographic investigations of cracked fillet weldments from various pressure vessel fabrications unlike simulated weldment fractures showed two distinct modes of crack propagation: (a) classical lamellar tearing; (b) abrupt brittle fracture.
2. Lamellar tearing constituted the primary (initial) mode of crack propagation followed by brittle fracture.
3. Thin, elongated manganese silicate and sulfide inclusions were found to be significantly influential in lamellar tearing.
4. The two modes of crack propagation lend themselves to the use of a fracture mechanics approach. Lamellar tearing can be conceived as the subcritical mode of crack propagation, and brittle fracture, the postcritical mode.
5. Engineering estimates of critical lamellar tear sizes made on the basis of fracture mechanics seem to agree fairly well with the fractographic observations.
6. Conventional tensile and Charpy V-notch tests performed in the through thickness direction of the plates offer suitable means of evaluating their susceptibility to weldment cracking. A screening criterion is developed for ASTM A515 Grade 65 carbon steel plates used in the weldments discussed in this paper.

References

1. Ferrar, J. C. M., and Dolby, R. E. 1969 (Feb.). Investigation into lamellar tearing. *Brit. Welding Inst.* 1.
2. Jubb, J. E. M. 1971. *Lamellar tearing.* WRC bulletin 168. New York: Welding Research Council.
3. Elliott, D. N. 1969. Fractographic examination of lamellar tearing in multi-run fillet welds. *Metal Constr. Brit. Welding Jnl.* 1(2S):50.
4. Elliott, D. N. 1969. Lamellar tearing in multiple fillet welds. *Welding Journal* 48(9):409-s to 416-s.
5. Heuschkel, J. 1971. Anisotropy and weldability. *Welding Journal* 50(3):110-s to 126-s.
6. Kihara, H., and Nishio, Y. 1973. *On the lamellar tearing in multiple fillet welds.* MHI Ltd. Pub.
7. Begley, J. A., and Logsden, W. A. 1971 (July). *Correlation of fracture toughness and Charpy properties for steels. W* scientific paper 71-1E7-MSLRF-P1.
8. Wessel, E. T. 1969. Linear elastic fracture mechanics for welded steel pressure vessels. *Practical fracture mechanics for structural steel.* UKAEA & Chapman & Hill.

WRC Bulletin 281
October, 1982

Hydrodynamic Response of Fluid Coupled Cylinders, Simplified Damping and Inertia Coefficients
by S. J. Brown

This study presents the development of the concept of inertia and damping coefficients in an historical context with experimental, classical and numerical investigations into the dynamics of fluid coupled cylinders. It is shown that coefficients may be used to account for coaxial cylinder end conditions, eccentricity, skewness, clusters, shell modes and axial modes.

Publication of this report was sponsored by the Subcommittee on Dynamic Analysis of Pressure Components of the Pressure Vessel Research Committee of the Welding Research Council.

The price of WRC Bulletin 281 is $11.50 per copy, plus $3.00 for postage and handling (foreign + $5.00). Orders should be sent with payment to the Welding Research Council, 345 E. 47th St., Room 1301, New York, NY 10017.

WRC Bulletin 282
November, 1982

Elastic-Plastic Buckling of Axially Compressed Ring Stiffened Cylinders—Test vs. Theory
by D. Bushnell

Concern for the safety of nuclear plants and offshore structures has stimulated efforts to determine buckling characteristics of stiffened cylindrical steel shells.

In this paper, BOSOR 5 computer programs were used to predict buckling loads of forty axially compressed mild steel cylindrical shells previously tested at Chicago Bridge & Iron Co.

Publication of this report was sponsored by the Subcommittee on Shells of the Pressure Vessel Research Committee of the Welding Research Council.

The price of WRC Bulletin 282 is $10.75 per copy plus $3.00 for postage and handling (foreign + $5.00). Orders should be sent with payment to the Welding Research Council, 345 E. 47th St., Room 1301, New York, NY 10017.